# Characterization of Combustion-Derived Individual Fine Particulates by Computer-Controlled Scanning Electron Microscopy

**Lian Zhang**
Dept. of Chemical Engineering, Monash University, Clayton Campus, VIC 3800, Australia

**Dunxi Yu, Hong Yao, and Minghou Xu**
State Key Laboratory of Coal Combustion, School of Energy and Power Engineering, Huazhong University of Science and Technology (HUST), Wuhan 430074, P.R. China

**Qunying Wang and Yoshihiko Ninomiya**
Dept. of Applied Chemistry, Chubu University, Kasugai, Aichi, Japan

*DOI 10.1002/aic.11922*
*Published online September 22, 2009 in Wiley InterScience (www.interscience.wiley.com).*

*Particulate matter (PM) emission from the combustion of solid fuels potentially poses a severe threat to the environment. In this article, a novel approach was developed to examine the properties of individual particles in PM. With this method, PM emitted from combustion was first size-segregated. Subsequently, each size was characterized by computer-controlled scanning electron microscopy (CCSEM) for both bulk property and single particle analysis. Combustion of bituminous coal, dried sewage sludge (DSS) and their mixture were conducted at 1200°C in a laboratory-scale drop tube furnace. Three individual sizes smaller than 2.5 μm were investigated. The results indicate that a prior size-segregation can greatly minimize the particle size contrast and phase contrast on the backscattered images during CCSEM analysis. Consequently, high accuracy can be achieved for quantifying the sub-micron particles and their inherent volatile metals. Regarding the PM properties as attained, concentrations of volatile metals including Na, K, and Zn have a negative relationship with particle size; they are enriched in the smallest particles around 0.11 μm as studied here. Strong interactions can occur during the cofiring of coal and DSS, leading to the distinct properties of PM emitted from cofiring. The method developed here and results attained from it are helpful for management of the risks relating to PM emission during coal-fired boilers.* © 2009 American Institute of Chemical Engineers *AIChE J,* 55: 3005–3016, 2009

*Keywords: CCSEM, size-segregation, sub-micron particles, volatile metals, modes of occurrence*

## Introduction

Particulate matter (PM) is a major pollutant formed during the combustion of coal and biomasses including sewage sludge.[1–3] Because of their small size and high specific

Correspondence concerning this article should be addressed to L. Zhang at lian.zhang@eng.monash.edu.au or Y. Ninomiya at ninomiya@isc.chubu.ac.jp

surface area, the particulates of 2.5 $\mu$m or less, namely $PM_{2.5}$, are rich in toxic metals. These particles have a high possibility of escaping conventional air control devices and hence causing adverse health impacts.[4,5] Extensive studies have confirmed that inhalation of $PM_{2.5}$ can give rise to a severe inflammatory reaction in lungs. The subcellular penetration of fine/ultrafine particles followed by localization in mitochondria can lead to oxidative stress.[6]

The properties of $PM_{2.5}$ are essential for the understanding of the formation of $PM_{2.5}$ as well as their environmental impacts. Specifically, the characteristics of individual particles have a close relationship with their health and environmental effects.[6] These characteristics include particle size, morphology, elemental composition, and oxidation states of heavy metals. In this regard, a number of advanced techniques have been used for PM characterization. Of those, electron microscopy is one of the most promising tools, including scanning electron microscopy (SEM), transmission electron microscopy (TEM) and computer-controlled scanning electron microscopy (CCSEM). Their applications for single particle analysis were critically reviewed.[7,8]

Characterization of particles by SEM or TEM is performed in a manual manner, which is thus readily biased by the analyst's ability to select the fields of view. Alternatively, CCSEM allows examining a large number of particles in an unattended run, in which properties of individual particles can be obtained simultaneously. Therefore, CCSEM has been used successfully for characterizing coarse ash particles,[9,10] combustion-derived PM with an aerodynamic diameter $\geq$2.5 $\mu$m,[11–13] and coarse PM emitted from a variety of natural sources.[14–21] Information is however scarce for particles in the sub-micron range. One reason is the intrinsic drawback of SEM-EDX. Its X-ray radiation can incur thermal damage upon fine particles, thereby causing subsequent mass loss for volatile elements such as S.[22,23] As a result, the quantifiable size is limited to 0.1–0.2 $\mu$m on the condition that a low-emission grid-supported carbon film is used as particle deposition substrate.[17–20]

The prior preparation of sample is another critical factor that can affect the validity of CCSEM data. A uniformly spatial distribution is essential for particles on the deposition substrate, whereas particle overlapping should be avoided.[11,16] In addition, CCSEM analysis relies on a preset grayscale image threshold to distinguish particles from the background. A fairly sharp threshold is essential for particle identification. However, combustion-derived $PM_{2.5}$ is a diverse mixture consisting of a wide range of sizes that have elemental and chemical compositions distinctively different from one another. Large particles and those rich in refractory metals such as Si, Al, and Fe appear bright on a backscattered electron (BSE) image, in contrast to the dim appearance of the particles rich in volatile elements and those in the sub-micron size range.[16,22] Both phase contrast and particle size contrast are mixed on a BSE image. Consequently, the small particles are readily biased by the larger ones in the case when they were collected together. The particles rich in light elements can also be biased by those containing heavy elements. All of these can result in a nonuniform distribution of particle signal, thus rendering it difficult to precisely set the CCSEM threshold.

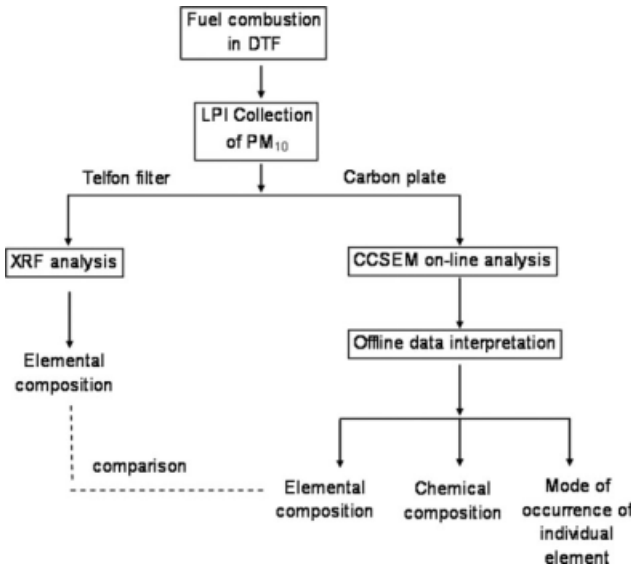


**Figure 1. Scheme of PM collection/size-segregation and characterization of individual sizes.**

To adequately reveal the properties of sub-micron particles in $PM_{2.5}$, a novel method was developed in this study, involving an initial size-segregation of $PM_{2.5}$ prior to CCSEM characterization. As explained in Figure 1, $PM_{2.5}$ emitted from a laboratory-scale drop tube furnace (DTF) was collected by a 13-stage low-pressure-impactor (LPI) that segregates particles into various size bins. This is expected to minimize the particle size contrast during later CCSEM analysis. Regarding CCSEM measurement, the bulk elemental composition of a size was first attained. Subsequently, CCSEM data were processed statistically to reveal the chemical compositions of discrete sizes as well as the modes of occurrence of the elements of interest. Three cases were studied: $PM_{2.5}$ emitted from the combustion of coal, dried sewage sludge (DSS) and their mixture. Special attention is given to the capability of CCSEM to elucidate the heterogeneity of particles in $PM_{2.5}$. Novel insights regarding the interactions among the metals of different single fuels are also anticipated, bearing significance in minimizing the environmental impacts of coal combustion.

## Experimental

### *Laboratory-scale combustion and $PM_{2.5}$ collection*

The solid fuels tested here were pulverized to $<$125 $\mu$m, including a bituminous coal, DSS and their mixture having a coal/DSS mass ratio of 50/50. As listed in Table 1, coal has more fixed carbon and less volatile matter than DSS. Silicon, aluminum, iron, and sulfur are abundant in coal ash, due to the prevalence of refractory mineral species such as alumino-silicates (e.g., kaolinite and quartz) and pyrite in high-rank coals. In contrast, DSS ash is rich in iron, calcium, and phosphorous, which are mostly derived from wastewater.

Combustion was conducted at 1200°C in air in a DTF as described elsewhere.[24] A solid fuel of about 0.2 g/min was entrained by primary air ($\sim$1 L/min) into the DTF. The preheated secondary air of $\sim$10 L/min was also fed into DTF.

**Table 1. Properties of the Fuels Tested in this Study**

| | Coal | DSS |
|---|---|---|
| Proximate analysis (wt %), dried | | |
| Moisture | 7.8 | 0.2 |
| Volatile matter | 24.7 | 47.3 |
| Fixed carbon | 54.7 | 32.3 |
| Ash | 12.8 | 20.2 |
| Elemental analysis (wt %), dry-and-ash-free | | |
| Carbon | 78.6 | 52.5 |
| Hydrogen | 4.9 | 6.4 |
| Nitrogen | 0.8 | 9.2 |
| Sulfur | 1.7 | 0.8 |
| Oxygen | 14 | 30.6 |
| Chlorine (ppm) | 270 | 5190 |
| Elemental composition of ash (wt %) | | |
| $SiO_2$ | 52.2 | 9.4 |
| $Al2O_3$ | 17.7 | 5.9 |
| $Fe_2O_3$ | 10.3 | 23.0 |
| CaO | 1.7 | 21.3 |
| MgO | 0.6 | 1.8 |
| $Na_2O$ | 0.3 | 1.5 |
| $K_2O$ | 1.4 | 2.9 |
| $SO_3$ | 15.4 | 11.3 |
| $P_2O_5$ | 0.4 | 23.0 |

The particle residence time was around 3 s. The burn-off rates are >95% for the three fuels.

A water-cooled and nitrogen-quenched sampling probe was installed at the bottom of DTF to collect the combustion products. The coarse particles were initially collected by two cyclones installed downstream of the sampling probe, with a cut-off size of around 2.5 $\mu$m. The exhaust gas was further diluted with clean air and directed into a 13-stage Andersen LPI for particle segregation. $PM_{2.5}$ was divided into nine narrow size bins having $d_{50}$ ranging from 2.5 $\mu$m down to <0.06 $\mu$m at the bottom of LPI.

Three sizes having $d_{50}$ of 2.5, 0.52, and 0.13 $\mu$m were characterized by CCSEM. Thin carbon plates with dimensions of $1 \times 1 \times 0.1$ $cm^3$ were used for particle deposition on the corresponding LPI stages. The collection time was <5 min, yielding a particle density lower than 30 $\mu g/cm^2$. Such a light loading can greatly minimize particle overlapping.[16] Furthermore, the three sizes were collected by Teflon filters for bulk analysis by X-ray fluorescence spectroscopy (XRF). The XRF results were used as reference to investigate if the selected observation fields of CCSEM are representative.

### *CCSEM analysis*

The particle-laden carbon plates were coated with an ultra-thin carbon layer, and subjected to a JEOL JSM-5600 CCSEM coupled with an EDAX-EDX spectrometer for single particle analysis. The analysis parameters are listed in Table 2.

For the size of 2.5 $\mu$m, a magnification of $\times$800 and particle size range of 2.0–4.6 $\mu$m were adopted considering that the particles collected on a LPI stage have a narrow size distribution around $d_{50}$, rather than a single size. For the other two sizes, a higher magnification of $\times$2000 was selected; the size ranges were selected as 0.3–1.0 and 0.1–0.5 $\mu$m for $d_{50}$ of 0.52 and 0.12 $\mu$m, respectively. Around 2000 particles were analyzed at each magnification, which is sufficient for statistical analyses.[16]

Special care was taken in the selection of fields of view during online CCSEM analysis, so as to avoid the particle overlapping under the deposition nozzle.[19] Moreover, the BSE images were further reviewed offline to preclude the overlapped aggregates that might be selected during the unattended CCSEM running. In the case that the large aggregates were selected, the corresponding fields of view were deleted. Additional fields were further chosen and measured. This sequence is crucial for the measurement of sub-micron particles, which was usually iterated several times to collect sufficient particles.

In each field of view the information stored on individual particles includes their position in the field, equivalent diameter/size, area, shape factor and elemental composition. The elemental compositions were corrected by the atomic number (Z)-dependent electron scattering, adsorption (A), and fluorescence (F) effects. The elements detected include O, Al, Si, Ca, Mg, S, Ti, Ba, Na, K, P, and Cl with K-alpha peak, and Zn with L-alpha peak. Their contents were normalized and carbon was precluded.

### *Offline interpretation on CCSEM data*

For quantification, the CCSEM data were initially processed using a statistical approach to reveal the bulk properties of individual sizes, including both elemental and chemical compositions. This is crucial for understanding the size-dependence of $PM_{2.5}$ properties. For chemical speciation, the classification scheme in Table 3 was adopted. Five major classes were considered: alumino-silicate compounds consisting of Si, Al, and/or alkali and alkaline earth metals (AAEM), phosphates, sulfates, chlorides, miscellaneous compounds containing more than three elements and the unknown that cannot be classified into any category. The density of each category is identical to the corresponding one in coal mineral classification.[25]

Regarding the mode of occurrence of an element, no statistical approaches were made because the number of particles containing some elements such as AAEM is deficient. Instead, it is presented in ternary diagrams in which the

**Table 2. Parameters for SEM and EDX Analysis**

| SEM | | EDX | |
|---|---|---|---|
| High tension | 15 kV | Magnification | $\times$800 for particulates with $d_{50}$ of 2.5 $\mu$m |
| Pressure | 0.9 torr | | $\times$2000 for particulates with $d_{50} \leq 1.0$ $\mu$m |
| Spot size | 15 | Particle size range | 1.0–4.6 $\mu$m at the magnification of $\times$800 |
| Image resolution | 1024 $\times$ 800 | | 0.5–2.0 $\mu$m at the magnification of $\times$2000 |
| | | Acquisition time | 15 s |
| | | Particle numbers | >2000 at each magnification |

**Table 3. CCSEM Species Classification Category, Based on EDX Analysis of the Elemental Composition of Single Particles (wt %)**

| Particle Category | | Density (g/cm$^3$) | Classification Rules Based on the Elemental Composition (wt %) |
|---|---|---|---|
| Alumino-silicates | Al-Si | 2.65 | Al + Si > 80, Si > 20, Al < 20 |
| | Si-rich | 2.65 | Si > 80 |
| | M-Al-Si | 2.80/2.60 | 15 < Al + Si < 90, P < 5, S < 5 |
| Phosphates | P-rich | 2.70 | P > 60, M < 5 |
| | M-P-O | 3.20 | 10 < P < 60, M > 5 |
| Sulfates | S-rich | 2.70 | S > 60 |
| | M-S-O | 2.50 | 10 < S < 50, M > 5, P < 5, Al + Si < 15 |
| chlorides | Na/K-Cl | 1.99 | Na/K + Cl > 60 |
| | Zn-Cl | 2.70 | Zn + Cl > 60 |
| Miscellaneous compounds | Al-Si-P-M | 2.70 | 15 < Al + Si < 60, P > 10, M > 5 |
| Others | | 2.70 | Unclassified compositions |

M represents a metal except Si and Al.

number percentage is plotted against particle composition on a three-element basis. Such a method can provide a valuable way of examining the associations among different elements.[13,26–28]

## Results and Discussion

### *Accuracy of CCSEM analysis*

Figure 2 demonstrates the results obtained from combustion of DSS, which are expressed in terms of comparison between CCSEM-determined elemental contents and that determined by XRF. Oxygen was not included. As indicated, the agreement between the two instruments is greatly dependent on both elemental type and particle size. Except for Fe in the sub-micron sizes, relatively good agreements were achieved for the refractory elements from Si to Mg and P. Fe in the sub-micron size was not detected by CCSEM, whereas XRF analysis revealed about 0.8 and 3.0 wt % of Fe in 0.55 and 0.12 $\mu$m, respectively.

Sulfur also has a significant mass loss during CCSEM analysis. Little of it was identified in the size of 2.5 $\mu$m, compared with around 3 wt % as determined by XRF. Regarding S in the medium size of 0.55 $\mu$m, CCSEM revealed about 8 wt % S, relative to ~16 wt % as determined by XRF. With particle size down to 0.12 $\mu$m, the deviation between two instruments however becomes smaller. Regarding the remaining volatile elements, their CCSEM-determined contents in the three sizes are rather consistent with the respective XRF results.

For further clarification, the accuracy of CCSEM analysis on a certain element (M) was evaluated by the ratio of its CCSEM-determined content ($M_{CCSEM}$) to that identified by XRF ($M_{XRF}$). The value of unity refers to an excellent accuracy. In contrast, a large deviation of the ratio from unity indicates low accuracy of CCSEM quantification. As evidenced in Figure 3, the refractory Si has ratios around 1.2–1.4 in three sizes, which are rather stable and less dependent on particle size. Its quantification errors are acceptable considering that the relative standard deviation (RSD) for major elements (>5 wt %) is around 20% for CCSEM analysis (private communication with Energy & Environmental Research Center, University of North Dakota, USA, Appendix A, Standard operating and sample preparation

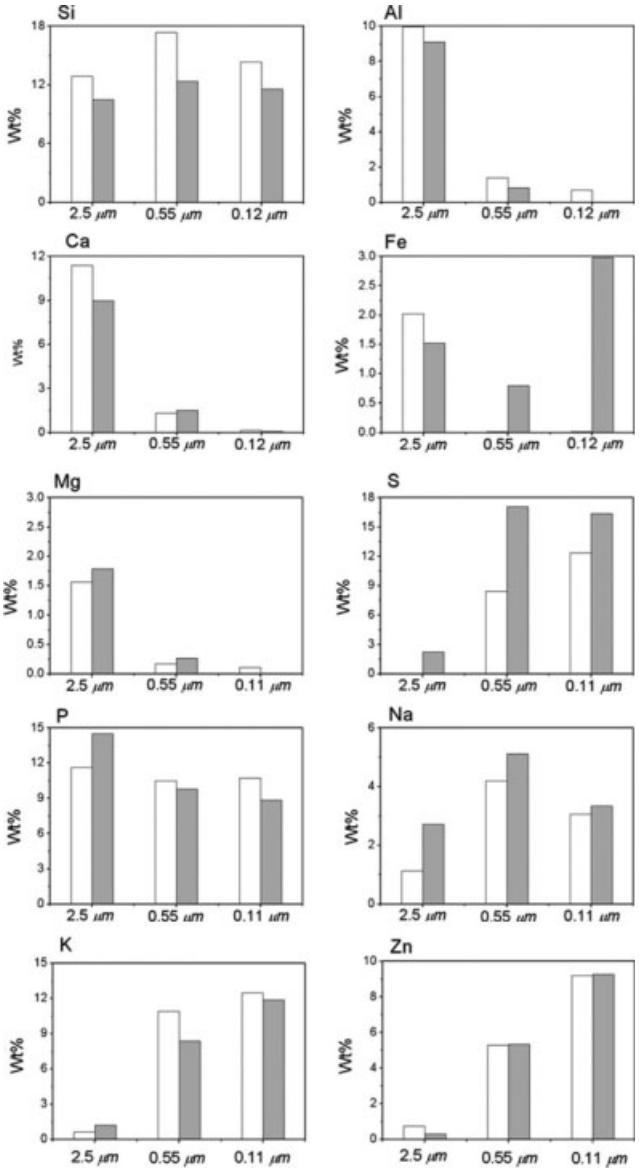


**Figure 2. Comparisons between the concentrations of major elements analyzed by CCSEM (white bars) and XRF (gray bars).**

PM was collected during DSS combustion.

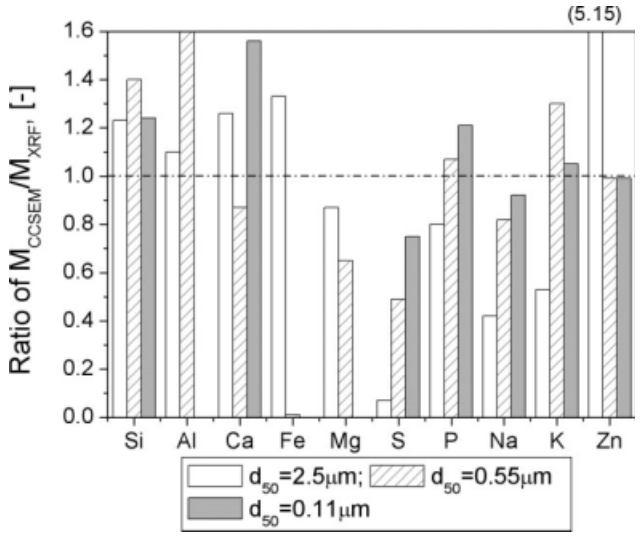


**Figure 3. Ratios between CCSEM-determined elements to the corresponding XRF-determined results.**

PM was collected from the combustion of DSS alone.

procedures). Al in the size of 2.5 $\mu$m has a similar ratio as well, while a larger value of about 1.6 was obtained for its presence in the medium size. No Al was detected in 0.11 $\mu$m. Similarly, Ca in the smallest size and Mg in the two sub-micron sizes also have large biases, which can be explained by their low concentrations. For CCSEM quantification, the minor species of 1–5 wt % usually have RSD around 40% (see private communication mentioned earlier). Regarding the large errors relating to Fe in the sub-micron particles, one explanation is the lower concentrations of Fe. Moreover, a nonuniform deposition of Fe-bearing particles could be formed on the substrate plate. Fe-bearing compounds are the heaviest species at a given size, which are thus preferentially concentrated under the deposition nozzles. They were mostly excluded upon the selection of CCSEM fields of view, as noted earlier.

The mass ratios of volatile elements from S to Zn show a strong dependence on particle size. With particle size decreasing, their mass ratios are much close to the unity. Especially for S, its mass ratio at 2.5 $\mu$m is only 0.1, which is however improved to 0.5 and then 0.8 with particle size down to 0.55 and 0.11 $\mu$m, respectively. Clearly, the volatile metals in the sub-micron range were quantified more accurately than in the larger size. This can be rationalized by the CCSEM threshold setting principle that the dominant phase on a BSE image is preferentially selected. For the large size of 2.5 $\mu$m, it is dominated by the refractory metals from Si to Mg having a total proportion >75 wt % (see XRF data in Figure 2). Thus, the minor metals that are volatile and light are largely overlooked. In contrast, with the particle size decreasing, the volatile metals tend to enrich, having a total amount comparable with the refractory metals in the medium size and even dominating the smallest size. Consequently, they can be easily distinguished and quantified more accurately.

The prior size-segregation of $PM_{2.5}$ is definitely the critical factor contributing to the high accuracy of CCSEM analysis on sub-micron particles. It greatly minimized the particle size contrast or phase contrast in a BSE image. No attempt was made to measure the whole $PM_{2.5}$ without size-segregation, it however can be inferred that, in the case that the three sizes were mixed together, the smaller particles and volatile metals within them could be underestimated in a manner similar to that confirmed for the volatile metals in 2.5 $\mu$m studied here. This is because particles larger than 1.0 $\mu$m are prevalent in $PM_{2.5}$, which usually have a mass greater than that of the sub-micron particles by a factor of 5–10.[29]

Approximately similar phenomena were observed for the other two cases including coal combustion alone and cofiring. Large errors were mainly observed for the minor metals in a certain size, due to the heterogeneity of each particle size as stated earlier.

### *Properties of particles with* $d_{50}$ *of 2.5 μm*

Irrespective of fuel type, this size is made up almost exclusively of refractory metals, as evidenced by the chemical compositions shown in Figure 4.

The Al-Si category is the most abundant species released from coal, including alumino-silicates such as mullite derived from the inherent clay minerals in coal.[13] A small amounts of Si-rich (quartz), Ca/Fe-Al-Si, and Na/K-Cl categories were also found, which could be generated by the direct liberation of inherent quartz, bursting of Ca/Fe-Al-Si liquid droplets and condensation of vaporized chlorides, respectively. Regarding particles emitted from DSS alone, the four-elemental Ca/Fe-P-Al-Si category is the most prevalent. It could have originated from the condensation of corresponding molten species. Cofiring released approximately equal quantities of Al-Si and Ca/Fe-P-Al-Si. The former species could be from coal, whereas the latter one may have a close relationship with particles from DSS.

The elemental compositions of Ca/Fe-P-Al-Si were further depicted as quasi-ternary diagrams. Al and Si are grouped together, namely Al + Si in the diagrams. Ca and Fe are grouped as Ca + Fe. Their percentages and that of P were

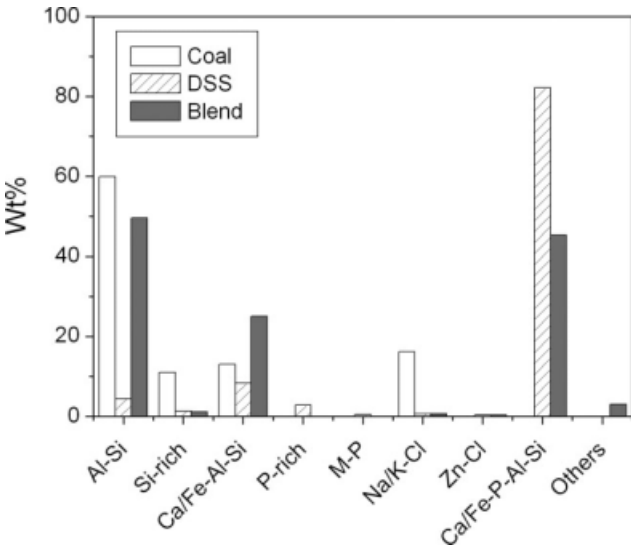


**Figure 4. Chemical compositions of particles having $d_{50}$ of 2.5 μm.**

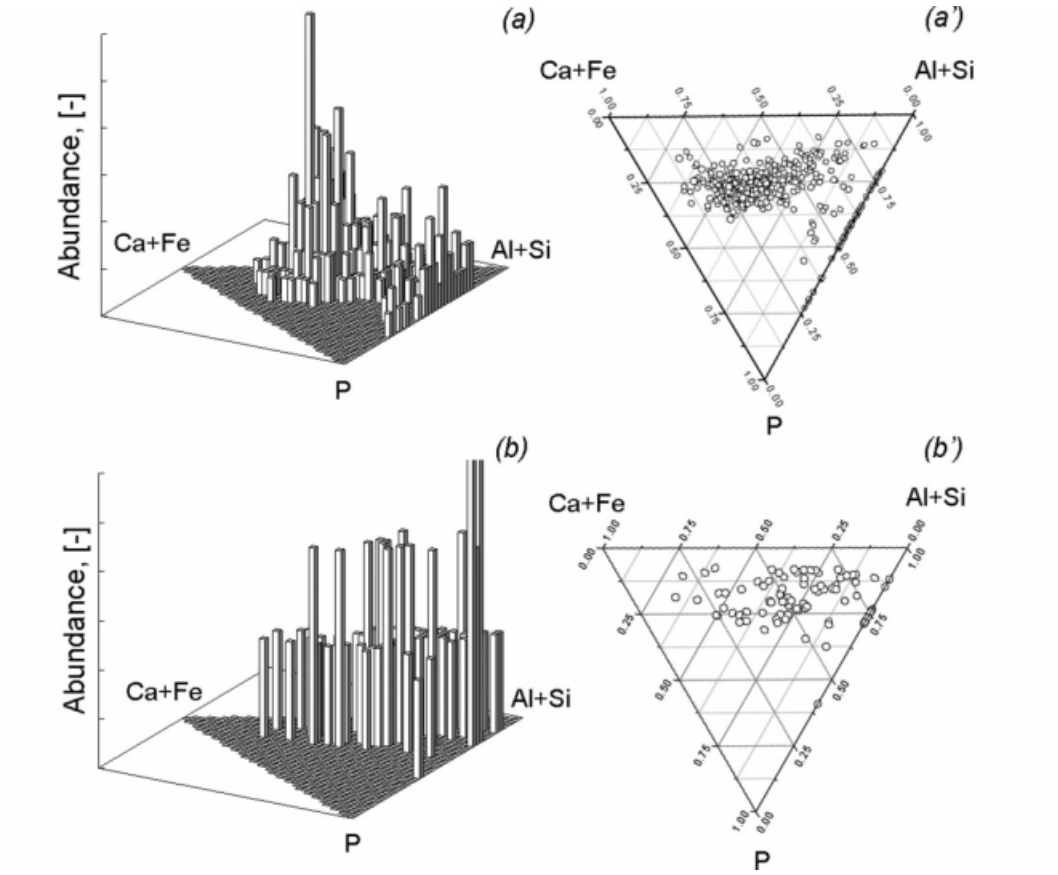


**Figure 5. Ternary diagrams for Al-Si-P-M complexes in the size of 2.5$\mu$m formed from combustion of DSS alone (a and a′) and the blend fuel (b and b′).**

normalized and illustrated as both abundance-ternary diagrams and standard ternary phase diagrams in Figure 5.

The DSS-derived particles have two major peaks including the particles containing four elements together and those containing no metals (Figures 5a, a′). The former group is rich in Ca and/or Fe, having a relatively narrow distribution in the mass ratio of these two metals to Al-Si. This category as well as the P-Al-Si species preferentially melted under given experimental conditions. P is a good network former to promote the formation of glassy ashes.[30] Strikingly, cofiring resulted in the great shift in the association among these four elements. Fewer particles were formed containing all of the four metals, whereas those having no metals are the most prevalent (Figures 5b, b′). In addition, nearly all of the particles shifted closer to the Ca + Fe-Al + Si line, indicative of less P in the complicated species released from cofiring. Obviously, cofiring led to notable interactions between the original minerals in single fuels. The original Ca/Fe and P in DSS could coagulate with coal ashes (e.g. Al-Si) to form aggregates larger than 2.5 $\mu$m. The shift rate of each element is however distinct. Compared with P, Ca and Fe could largely incorporate into coal-derived alumino-silicates, thereby mostly shifting into the coarse particles. P could however be partly adsorbed as gaseous vapor on the surface of coal-derived fine Al-Si, thus remaining in $PM_{2.5}$.

### *Properties of particles with* $d_{50}$ *of 0.55 $\mu$m*

For this size emitted from a combustion source, it exhibits different chemical composition to those of 2.5 $\mu$m. The fuel

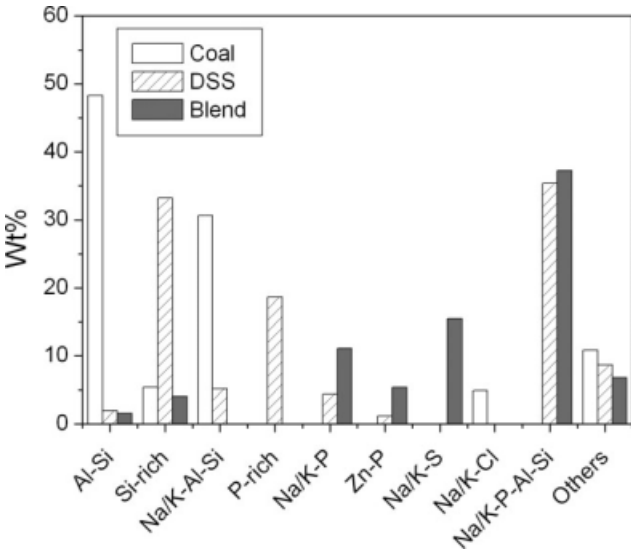


**Figure 6. Chemical compositions of particles having $d_{50}$ of 0.52 $\mu$m.**

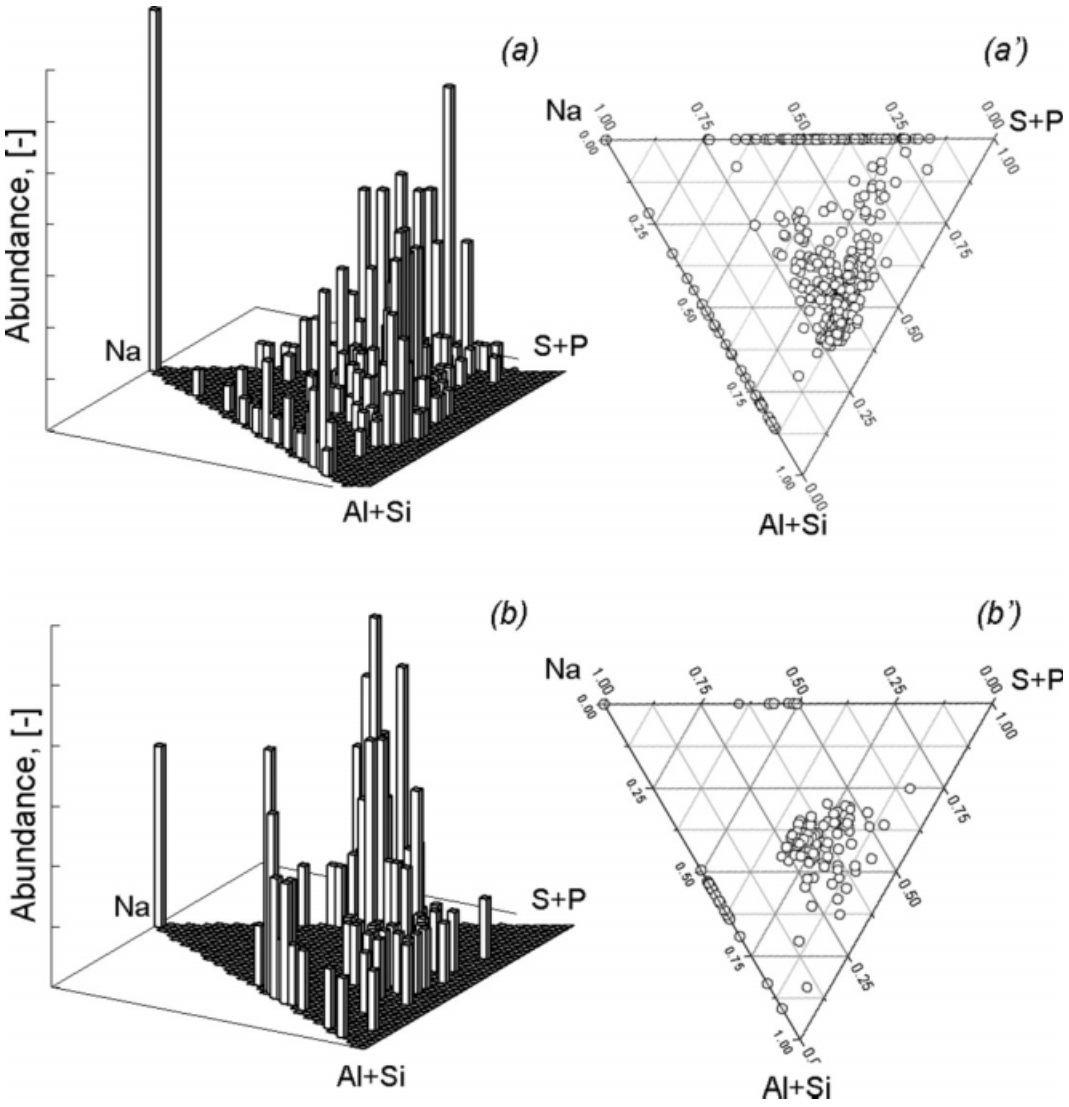


**Figure 7. Na-(S + P)-(Al + Si) ternary diagrams.**

Panels (a) and (a′) are the results obtained from DSS alone combustion; (b) and (b′) are from cofiring. All particles have a $d_{50}$ of 0.55 $\mu$m.

type also plays an important role. As illustrated in Figure 6, Al-Si is still the most abundant category derived from coal combustion. Na/K-Al-Si was formed as well, which is however deficient in 2.5 $\mu$m. Clearly, Na and K are enriched in the sub-micron particles, likely due to the capture of their gaseous portions on solid alumino-silicates.

DSS alone released a wide variety of categories. The Na/K-P-Al-Si complex is the most prevalent, followed by Si-rich, P-rich, and others in decreasing order. Although the refractory metals still dominate, more Na and K and P are clearly condensed in this size. P-rich can be the aggregated $P_2O_5$ nuclei generated from oxidation of gaseous P vapor, or organic-P adsorbed on the unburnt carbon. The four-elemental Na/K-P-Al-Si complex can be formed in a manner to that of Na-Al-Si released from coal. Solidification of its molten droplets contributes to the sub-micron particle formation.

Cofiring exerts a profound effect on this size as well, yielding the distinct modes of occurrence of metals within it. Apart from the prevalence of Na/K-P-Al-Si complex, new categories such as Na/K-P and Na/K-S were also formed. Meanwhile, the proportions of coal-derived Al-Si and Na/K-Al-Si and DSS-derived P-rich were greatly reduced. This further suggests interactions among different elements during cofiring, including:

$$\text{Phosphation} \quad M_{(g)} + P_{(g)} + O_{2(g)} \rightarrow M_x(PO_4)_{y(s)} \tag{1}$$

$$M_xO_{(s)} + P_2O_{5(g)} + O_{2(g)} \rightarrow M_x(PO_4)_{y(s)} \tag{2}$$

$$\text{Sulfation} \quad M_xO_{(s)} + SO_{2(s)} + O_{2(g)} \rightarrow M_x(SO_4)_{y(s)} \tag{3}$$

$$\text{Coagulation} \quad M_x(PO_4)_{y(s)} + Al_2O_3 \cdot SiO_{2(s)} \rightarrow M_xO \cdot (P_2O_5)_{y/2} \cdot (Al_2O_3 \cdot SiO_2)_{z(l)} \tag{4}$$

M represents a gaseous element such as Na, K, or Zn. The former two elements, especially K are likely released from two single fuels, whereas Zn is mostly from DSS. P is also

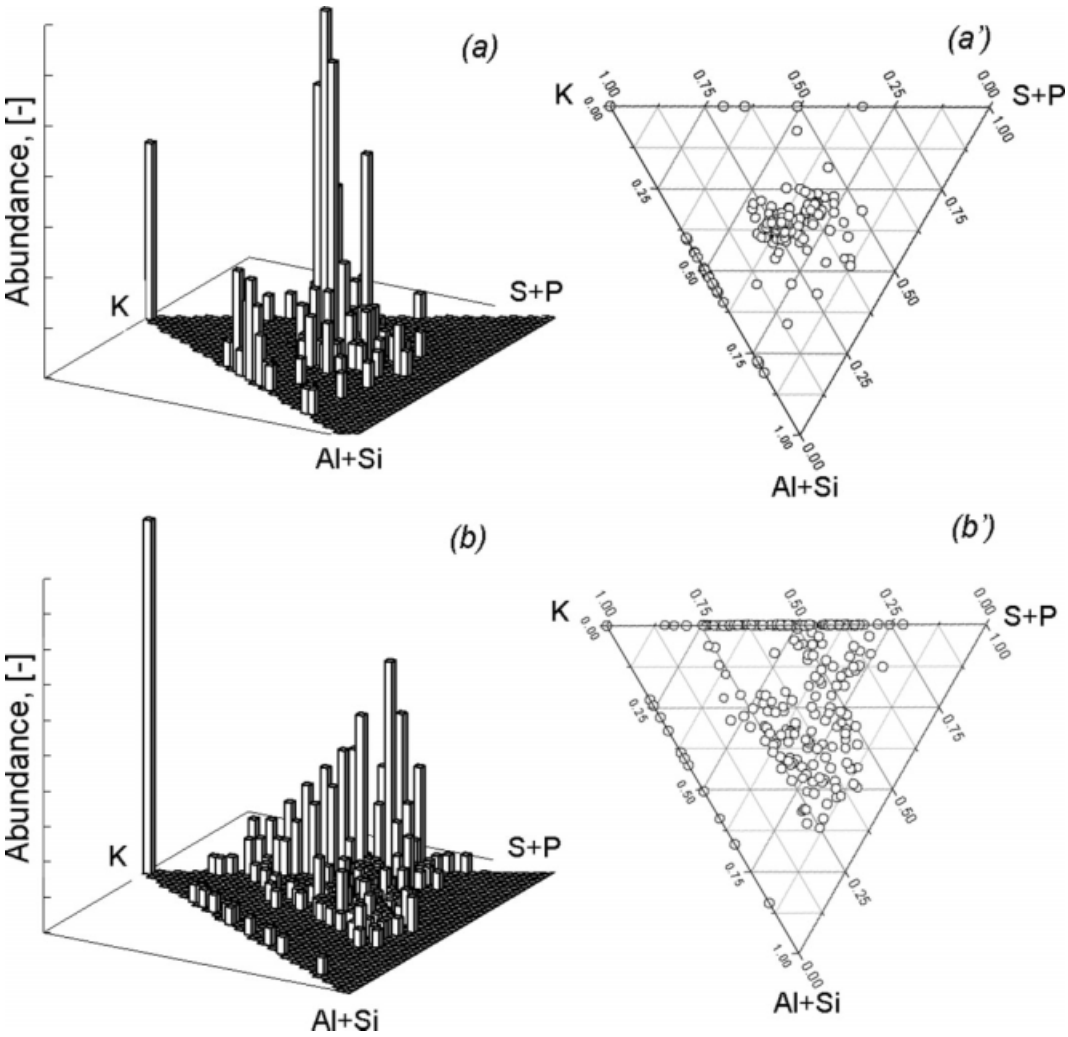


**Figure 8. K-(S + P)-(Al + Si) ternary diagrams.**

Panels (a) and (a′) are results obtained from DSS alone combustion; (b) and (b′) are results from cofiring. All particles have a $d_{50}$ of 0.55 $\mu$m.

mostly derived from DSS. $SO_2$ however mainly comes from coal combustion, considering that coal is rich in sulfur when compared with DSS (Table 1).

The mode of occurrence of a volatile metal can be greatly affected by these reactions. This in turn influences its properties including water-solubility and toxicity. In this respect, the modes of occurrence of the three elements were expressed as ternary diagrams in Figures 7–9. Note that the results for combustion of coal alone were not considered here due to less volatile elements released from coal.

As demonstrated in Figure 7, Na emitted from DSS alone is mostly present in the corner unbound to other elements, which can be assigned as sodium oxide and/or chloride (Figures 7a and a′) that were formed from the condensation of their gaseous phases. The next most abundant species is the water-soluble Na-S/Na-P category. Cofiring however caused more Na to be shifted towards the categories containing both Al-Si and Na. They could be formed by the capture of Na-bearing vapors or its oxide nuclei by coal-derived Al-Si, as noted before. Na is one vaporized metal whose partitioning between vapor and solid is greatly determined by its proximity to alumino-silicate compounds.[31]

K and Zn behaved differently to Na. For K released by DSS alone, its most probable species is the four-elemental complex (Figures 8a, a′). On the other hand, cofiring released more pure K and those containing K and S/P together. Such a shift is converse to that of Na. A similar phenomenon occurred for Zn (Figure 9). Clearly, More of K and Zn in this size are water soluble, thus posing higher environmental risks.

### *Properties of particles with* $d_{50}$ *of 0.11 μm*

This smallest size shows the greatest volatile metal enrichment, containing a large number of particles generated from the condensation of gaseous species. The properties of this size also exhibit a strong fuel-dependence.

The particles emitted from coal alone are composed of P-rich, S-rich, Na/K-S, and Na/K-P categories (Figure 10). Here again, the former two categories can be assigned as

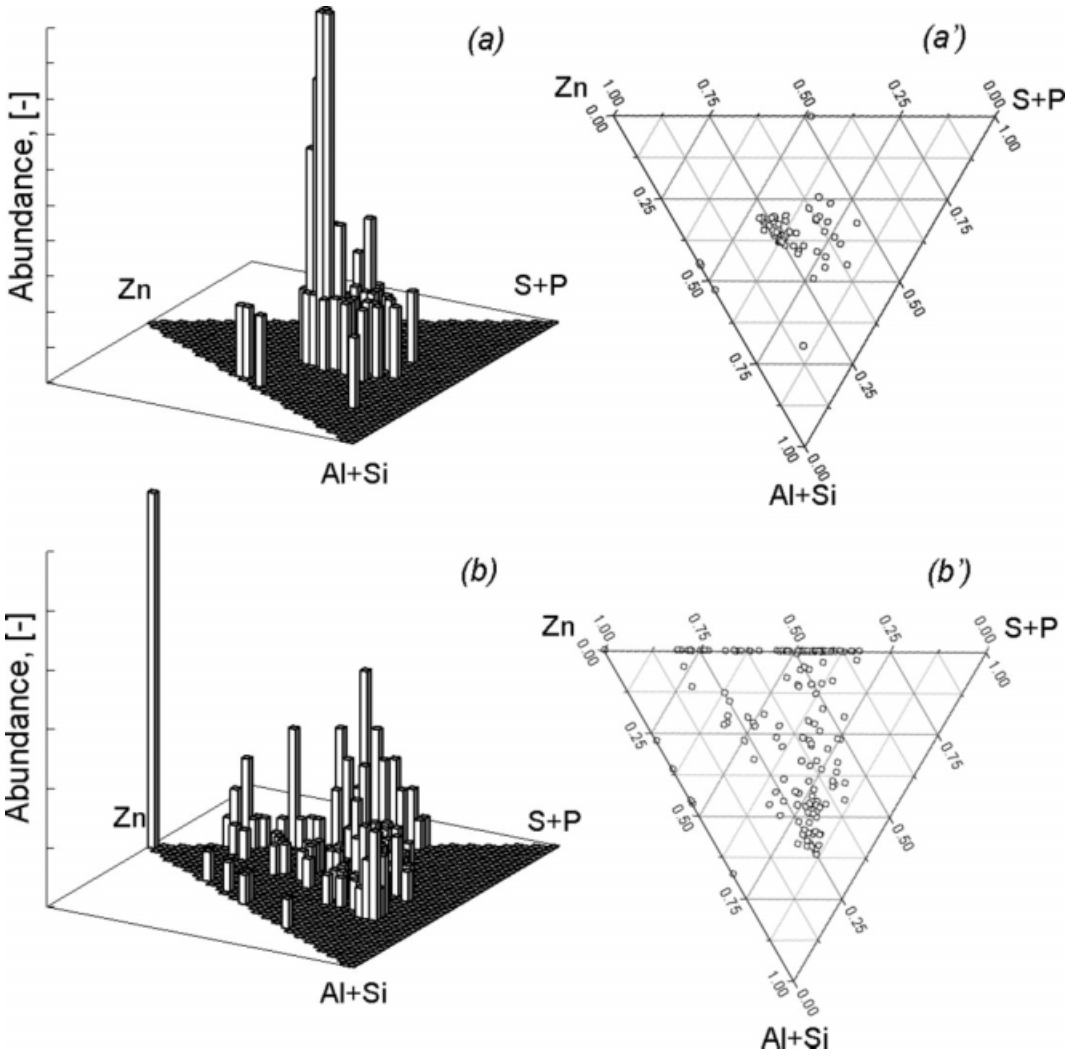


**Figure 9. Zn-(S + P)-(Al + Si) ternary diagrams.**

Panels (a) and (a′) are results obtained from DSS alone combustion; (b) and (b′) are results from cofiring. All particles have a $d_{50}$ of 0.55 $\mu$m.

condensed $P_2O_5$, sulfur mist and/or their organic fractions adsorbed on the unburnt carbon, whereas the latter two are assignable to sulfates and phosphates, respectively. DSS combustion released distinctively different categories. Si is mostly associated with elements including Na, K, and P to form silicates and multielemental complexes. Silicates can be formed from the homogeneous interaction between metallic vapors and vaporized silicon (Si)/silicon suboxide (SiO). Other species were also formed, including phosphates (P-rich, Na/K-P, and Zn-P categories), sulfates (Na/K-S and Zn-S), and chlorides (Na/K-Cl and Zn-Cl).

Cofiring resulted in significant shift in the chemical compositions. Fewer Si-containing or P-bearing compounds while more sulfates and chlorides were formed from cofiring. Clearly, both Si and P shifted to the larger particles, due to their coalescence with other species. Formation of a large quantity of Zn-S corresponds with the reduction of the S-rich category, further suggesting interactions between DSS-derived Zn and coal-derived $SO_2/SO_3$. This finding is also consistent with that found for the particles around 0.55 $\mu$m.

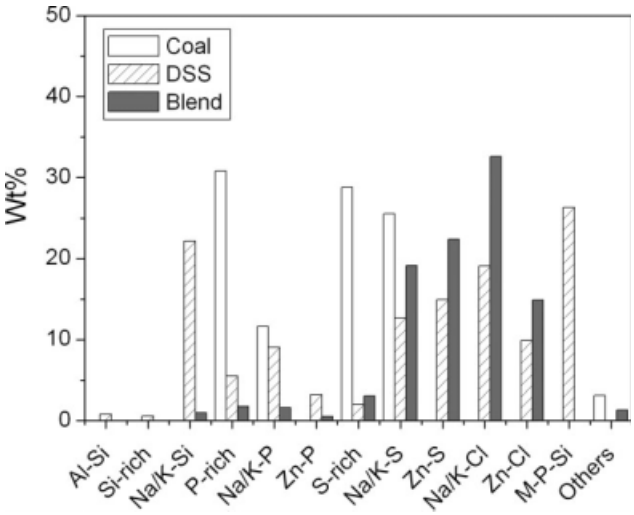


**Figure 10. Chemical compositions of particles having $d_{50}$ of 0.11 $\mu$m.**

The formation of Na/K-Cl and Zn-Cl categories is interesting. Their presence in $PM_{2.5}$ is assigned as those formed from condensation of gaseous chlorides in the sampling probe, rather than particles formed in situ in the reactor, because the boiling points for chlorides are lower than the reaction temperature adopted here. Nevertheless, their quantities and detailed elemental compositions are helpful to reveal the volatilization of these elements during combustion.

As evidenced by the Na-K-Cl ternary diagrams in Figure 11, Cl is mostly bound with Na and present in the form of NaCl during the combustion of DSS alone, while less KCl was found. This implies the presence of original NaCl in DSS, which has high vaporization potential and can evaporate preferentially in a combustion system. Cofiring however resulted in the formation of a large amount of KCl.

In combination with the results found for the medium size, this finding further confirms the correlation between Na behavior and that of K during cofiring. As indicated elsewhere,[31] in the case that Na and Cl coexist in a typical combustion environment, the mobile Na is able to displace mineral-bound K such as illite, which would not otherwise be expected to vaporize. Once mobilized, the gaseous K could further react with Cl, S, and/or P and condense into submicrometer particles.

The proportions of both Zn-Cl and Zn-S categories emitted from cofiring are higher than the respective results of single fuels. These changes can be explained by the decreasing of other species such as refractory Al-Si in this size. Effect of cofiring is not obvious.

### *General discussion*

A prior size-segregation can greatly minimize the particle size contrast and phase contrast that are often encountered in the conventional CCSEM measurement. As a consequence, the sub-micron particles and their inherent volatile metals can be quantified in a fairly accurate sense. By measuring about 2000 particles, the accurate bulk properties of a certain size can be attained. More importantly, an enormous amount of information can be achieved for individual particles. Therefore, the distribution of an element in $PM_{2.5}$ and its mode of occurrence are deduced statistically. This feature is unavailable in conventional CCSEM and other techniques.

Case studies here further confirm the significance of the developed method. Although only three sizes were analyzed, insights can still be gained into the chemical and physical reactions that take place among the inorganic elements. The vaporized metallic vapors preferentially condense into submicron particles, which can also be partly captured by the refractory mineral species. Cofiring of coal with DSS greatly affects the fates of volatile elements. As demonstrated here, a portion of the coal-derived mineral-bound K could be mobilized by the DSS-derived Na. Consequently, a large quantity of KCl was emitted from cofiring. Sulfur derived from coal, however, was capable of attacking the DSS-derived gaseous Zn to form zinc sulfate that potentially condensed into sub-micron particles. Such a finding is consistent with what is reported elsewhere.[32,33] In addition, the phosphorous derived from DSS promoted the agglomeration among mineral species. Clearly, these reactions can significantly affect the operation of a utility boiler where cofiring is expected to replace conventional coal combustion. Special care should thus be taken with the erosion and corrosion problems related to molten sulfates and phosphates. Furthermore, these results are helpful for an accurate evaluation of the environmental impacts of $PM_{2.5}$. Apart from bulk property analysis, direct evidence can also be obtained through CCSEM analysis on the modes of occurrence of potentially toxic elements, particularly those in the sub-micron size range. The resulting information is crucial for the evaluation of water-solubility of $PM_{2.5}$ as well as its toxicity and environmental impacts.

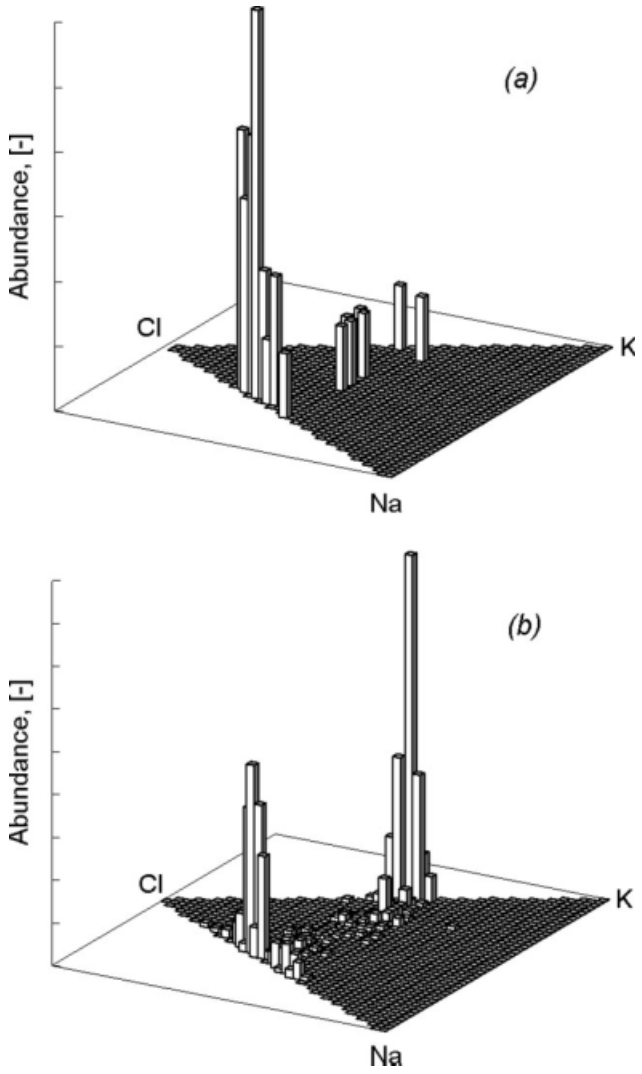


**Figure 11. Na-K-Cl ternary diagrams.**

Panel (a) is the result obtained from DSS alone combustion and (b) is from cofiring. All particles have a $d_{50}$ of 0.11 $\mu$m.

## Conclusions

Combining a prior size-segregation with CCSEM analysis is a promising method to determine the properties of individual particles in the $PM_{2.5}$ emitted from coal combustion and cofiring. A study of $PM_{2.5}$ emitted from three combustion sources led to the following conclusions.

1 Size-segregation of $PM_{2.5}$ by LPI is capable of reducing the particle size contrast and phase contrast on BSE images during CCSEM analysis. Accordingly, the dominant phase in a certain size was quantified with an RSD around 20% or less. Especially, the sub-micron particles and volatile metals within them were measured precisely. In terms of the bulk elemental composition, CCSEM compared favorably with other methods such as XRF.

2 The obvious interactions among the elements of single fuels occurred during cofiring. P, Ca, and/or Fe in DSS coalesced with coal-derived refractory minerals into coarse ash particles. DSS-derived Zn was sulfated by S from coal to form zinc sulfate in $PM_{2.5}$. On the other hand, the refractory mineral-bound K in coal could be mobilized by Na from DSS, transforming into chloride during cofiring.

3 The results for sub-micron particles are helpful for understanding the influence of cofiring on their emissions. Insights can also be gained for the modes of occurrence of volatile metals and their environmental impacts.

## Acknowledgements

This work was supported by Japan Society for the Promotion of Sciences (JSPS), Ministry of Education, Science, Sports and Technology of Japan for scientific research on priority areas (B) 20310048, and State Key Laboratory of Coal Combustion, Huazhong University of Science and Technology under its opening foundation (No. 200701), and the Program of Introducing Talents of Discipline to Universities ("111" project No.B06019), China. Part of this work was presented at the 21st International Pittsburgh Coal Conference, September 13–17, 2004, Osaka, Japan.

## Notation

### *Nomenclature*

AAEM = alkali and alkaline earth metals
BSE = backscattered electron
CCSEM = computer-controlled scanning electron microscopy
$d_{50}$ = diameter of the particle having a 50 percent collection efficiency
DSS = dried sewage sludge
DTF = drop tube furnace
EDX = energy dispersive X-ray analysis
LPI = low-pressure impactor
M = an element
$M_{CCSEM}$ = content of an element quantified by CCSEM
$M_{XRF}$ = content of an element quantified by XRF
PM = particulate matter
$PM_{2.5}$ = particulates with an aerodynamic diameter smaller than 2.5 $\mu$m
$PM_{10}$ = particulates with an aerodynamic diameter smaller than 10 $\mu$m
RSD = relative standard deviation
SEM = scanning electron microscopy
TEM = transmission electron microscopy
XRF = X-ray fluorescence spectroscopy

### *Roman symbols*

Al + Si = the sum of concentrations of aluminum and silicon
Ca + Mg = the sum of concentrations of calcium and magnesium
S + P = the sum of concentrations of sulfur and phosphorous

### *Subscripts*

(g) = gas
(l) = liquid
(s) = solid
$x$, $y$, $z$ = stoichiometric moles of an atom

## Literature Cited

1. Smith IM, Sloss LL. *$PM_{10}$/$PM_{2.5}$—emissions and effects*. *IEA Coal Research*, London, United Kingdom, 1998.
2. Nelson PF. Trace metal emissions in fine particles from coal combustion. *Energy Fuels*. 2007;21:477–484.
3. Seames WS, Fernendez A, Wendt JOL. A study of fine particulate emissions from combustion of treated pulverized municipal sewage sludge. *Environ Sci Technol*. 2002;36:2772–2776.
4. Lockwood FC, Yousif S. A model for the particulate matter enrichment with toxic metals in solid fuel flames. *Fuel Process Technol*. 2000;65–66:439–457.
5. Lighty JS, Veranth JM, Sarofim AF. Combustion aerosols: factors governing their size and composition and implications to human health. *J Air Waste Manage Assoc*. 2000;50:1565–1618.
6. Chen YZ, Shah N, Huggins FE, Huffman GP. Transmission electron microscopy investigation of ultrafine coal fly ash particles. *Environ Sci Technol*. 2005;39:1144–1151.
7. Jambers W, Bock LD, Grieken RV. Recent advances in the analysis of individual environmental particles. *Rev Analyst*. 1995;120:681–692.
8. Watt J. Automated characterization of individual carbonaceous fly-ash particles by computer-controlled electron microscopy: analytical methods and critical review of alternative techniques. *Water Air Soil Pollut*. 1998;106:309–327.
9. Gupta RP, Wall TF, Kajigaya I, Miyamae S, Tsumita Y. Computer-controlled scanning electron microscopy of mineral in coal—implications for ash deposition. *Prog Energy Combust Sci*. 1998;24:523–543.
10. Yu D, Xu M, Zhang L, Yao H, Wang Q, Ninomiya Y. Computer-controlled scanning electron microscopy (CCSEM) investigation on the heterogeneous nature of mineral matter in six typical Chinese coals. *Energy Fuels*. 2007;21:468–476.
11. Casuccio CS, Schlaegle ST, Lersch TL, Huffman GP, Chen YZ, Shah N. Measurement of fine particulate matter using electron microscopy techniques. *Fuel Process Technol*. 2004;85:763–779.
12. Cprek N, Shah N, Huggins FE, Huffman GP. Computer-controlled scanning electron microscopy (CCSEM) investigation of quartz in coal fly ash. *Fuel Process Technol*. 2007;88:1017–1020.
13. Chen YZ, Shah N, Huggins FE, Huffman GP, Linak WP, Miller CA. Investigation of primary fine particulate matter from coal combustion by computer-controlled scanning electron microscopy. *Fuel Process Technol*. 2004;85:743–761.
14. Lorenzo R, Kaegi R, Gehrig R, Grobéty B. Particle emissions of a railway line determined by detailed single particle analysis. *Atmos Environ*. 2006;40:7831–7841.
15. Jambers W, Grieken RV. Single particle characterization of inorganic suspension in lake Baikal, Siberia. *Environ Sci Technol*. 1997;31:1525–1533.
16. Mamane Y, Willis R, Conner T. Evaluation of computer-controlled scanning electron microscopy applied to an ambient urban aerosol sample. *Aerosol Sci Technol*. 2001;34:97–107.
17. Laskin A, Gaspar DJ, Iedema MJ, Cowin JP. *Exploring single-particle heterogeneous chemistry of aerosols using SEM, CCSEM, ESEM, and TOF-SIMS analytical techniques, Combustion and atmospheric pollution. Proceedings of the International Symposium on Combustion and Atmospheric Pollution*. St. Petersburg, Russia, 2003:565–569.
18. Laskin A, Wietsma TW. Heterogeneous chemistry of individual mineral dust particles with nitric acid: a combined CCSEM/EDX, ESEM, and ICP-MS study. *J Geophys Res*. 2005;110:D10208, doi:10.1029/2004JD005206, 1–15.
19. Laskin A, Iedema M, Cowin JP. Time-resolved aerosol collector for CCSEM/EDX single-particle analysis. *Aerosol Sci Technol*. 2003;37:246–260.
20. Laskin A, Iedema MJ, Cowin JP. Quantitative time-resolved monitoring of nitrate formation in sea salt particles using a CCSEM/EDX particle analysis. *Environ Sci Technol*. 2002;36:4948–4955.
21. Kennedy SK, Walker W, Forslund B. Speciation and characterization of heavy metal-contaminated soils using computer-controlled scanning electron microscopy. *Environ Forensics*. 2002;3:131–143.
22. Poelt P, Mitsche S, Brunner T, Schmied M. Automated analysis of submicron particles by CCSEM/EDXS-where are the limits? *Inst Phys Conf Ser*. 1999;168:81–84.
23. Schmied M, Poelt P. Particle analysis by SEM/EDXS and specimen damage. *Mikronchim Acta*. 2002;139:171–177.

24. Zhang L, Sato A, Ninomiya Y. CCSEM analysis of ash from combustion of coal added with limestone. *Fuel*. 2002;81:1499–1508.
25. Huggins FE, Kosmack DA, Huffman GP, Lee RJ. Coal mineralogies by SEM image analysis. *Scanning Electron Microsc*. 1980;1:531–540.
26. Zhang L, Wang Q, Sato A, Ninomiya Y, Yamashita T. Interactions among inherent minerals during coal combustion and their impacts on the emission of $PM_{10}$: 2. Emission of submicrometer-sized particles. *Energy Fuels*. 2007;21:766–777.
27. Zhang L, Masui M, Mizukoshi H, Ninomiya Y, Kanaoka C. Formation of submicron particulates ($PM_1$) from the oxygen-enriched combustion of dried sewage sludge and their properties. *Energy Fuels*. 2007;21:88–98.
28. Shah A, Huffman GP, Huggins FE, Shah N, Helble JJ. Behavior of carboxyl-bound potassium during combustion of an ion-exchanged lignite. *Fuel Process Technol*. 1995;44:105–120.
29. Wang Q, Zhang L, Sato A, Ninomiya Y, Yamashita T. Interactions among inherent minerals during coal combustion and their impacts on the emission of $PM_{10}$. I. Emission of micrometer-sized particles. *Energy Fuels*. 2007;21:756–765.
30. Zhang L, Ninomiya Y. Transformation of phosphorous during combustion of coal and sewage sludge and its contributions to $PM_{10}$. *Proc Combust Inst*. 2007;31:2847–2854.
31. Linak WP, Wendt JOL. Toxic metal emissions from incineration: mechanisms and control. *Prog Energy Combust Sci*. 1993;19:145–185.
32. Fernandez A, Wendt JOL, Witten ML. Health effects of coal and biomass combustion particulates: influence of zinc, sulfur, process changes on potential lung injury from inhaled ash. *Fuel*. 2005; 84(10):1320–1327.
33. Fernandez A, Davis SB, Wendt JOL, Cenni R, Young RS, Witten ML. Public health-particulate emission from biomass combustion. *Nature*. 2001;409(6823):998–998.

*Manuscript received July 3, 2008, and revision received Mar. 15, 2009.*